Indian Journal of Biochemistry & Biophysics
Vol. 60, January 2023, pp. 7-25
DOI: 10.56042/ijbb.v60i1.56987

# A comparative computational approach on the most deleterious missense variant in Connexin 43 protein and its potent inhibitor analysis

Ramkumar Katturajan[1], Tamma Medha[1], Sakshi Karra[1], Vidya R[2] & Sabina Evan Prince[1]*

[1]Department of Biomedical Sciences, School of Biosciences and Technology; & [2]VIT School of Agri innovations and Advance Learning (VAIAL), VIT Vellore-632 014, Tamil Nadu, India

*Received 09 November 2021*; *revised 09 December 2022*

Intercellular communication between the cell plays an essential role in cell growth and cell formation, including migration, metabolism, and cell differentiation. Cell function and tissue homeostasis are maintained through gap junction intercellular communication (GJIC), thus regulating connexin hemichannels. Mis regulation of such connexin, especially connexin (Cx) 43, affects a comprehensive process, including cell differentiation, inflammation, and cell death. Mis regulation may be due to the missense variant in Cx43. Thus, we screened the complete set of mutations from public mutational databases and obtained 219 missense variants, which were then classified based on their pathogenicity, functional impact, stability, conservation, and physiochemical properties. Variant L214P was scrutinized to have the most deleterious, which was then modelled using the I-TASSER server and performed molecular docking analysis to screen potent inhibitors. The compound Kanamycin, Ginsenoside, and Astragaloside IV have better interactions with Cx43 mutant with a maximum of 5 hydrogen bonds. Ginsenoside is a compound that follows a Lipinski rule of five. Thus, the result obtained from this study suggests that Ginsenoside would be a better potent inhibitor for native and mutant Cx43.

**Keywords**: Cx43, L214P, Virtual screening, Variant classification, Molecular docking

Connexins (Cxs) are a multi-gene family of proteins that regulate the intercellular hole intersection of gap junction (GJ) channels to coordinate communication amongst cells[1]. GJ channels are shaped by the docking of two hemichannels, one from each of the two reaching cells. It is presently well established that each hemichannel can work with the nonappearance of docking and subsequently intervening signaling across the plasma film[2]. GJ channels of Hemi channels play an essential role in many aspects of tissue homeostasis within the brain, heart, and other tissues, as evidenced by the link between a growing list of human illnesses and changes in connexin characteristics[3]. It is fundamental for some physiological cycles, like coordinated depolarization of cardiac muscle, proper embryonic development, and the conducted response in the microvasculature.

Consequently, transformations in connexin-encoding qualities can prompt functional and formative anomalies. Twenty-one different Cxs have been identified and studied, which consist of four transmembrane helices (TM1-TM4), two extracellular loops (ECL1 and ECL2), an N-terminal helix, and a large carboxy-terminal domain[4]. Among all the Cxs, Cx43 is widely distributed in almost all the cell types in most organs and is significantly expressed under disease conditions[5].

Under stress situations, the activity of the hemi channels changes that are entailing moving molecules such as $Ca2^{+}$, ATP, $NAD^{+}$, and glutamate to another cell and inducing numerous physiological responses[5]. Mutations in 10 different human Cxs have been related to 28 hereditary disorders. Cx43 mutations were responsible for more than six illnesses[3]. As a result, many mechanistic studies have been conducted on this Cx43. Concerning the importance of Cxs mutations, connexinopathies have been identified, termed diseases related to the Cxs mutations. Mutations in Cx43 were reported to have several genetic disorders, including oculodentodigital dysplasia, palmoplantar keratoderma, congenital alopecia, hyperkeratosis, leukonychia, erythron-keratodermia variabilis et progressive and linear verrucous epidermal nevus[6-8]. In addition, Cx43 mutations are also associated with several heart diseases where the principal role of Cx43 in the myocardium is to regulate the rapid and coordinated excitation-contraction coupling mechanisms[9].

*Correspondence:
Phone: 91-416-2202324; +91-9080494445 (Mob)
E-mail: eps674@gmail.com; epsabina@vit.ac.in

Moreover, several reports have suggested that Cx43 mutants lack a C-terminal tail which results in inhibited cell division and failure to form GJ shown to have down regulated cell growth[10]. Nonetheless, there is literature to assist in identifying the most harmful or significant mutations responsible for disease causation and development[11]. Rangasamy *et al*., 2021 has recently reported that computational approach to predict mutations are essential in scrutinizing the most significant disease-causing mutation[12].

The computational design approach comprises virtual screening and molecular docking that has manifested trustable evidence in drug developments and definite outcomes[13,14]. Cx43 has been of foremost importance in various disease conditions, and the significance of the related mutations has been analyzed using various web-based tools. The present study examines the first analysis of the mutational landscape of Cx43 in association with a virtual screening of Cxs inhibitors on most pathogenic mutation L214P. Primarily, we screened the complete set of mutations from mutational databases and classified them based on their pathogenicity, functional impact, stability, conservation, and physiochemical properties. A native and mutant model with the desired variation was modeled using the I-TASSER server, and the Cx inhibitor was screened based on the literature survey (Table 4). Molecular docking was performed to find the potent desired Cx43 mutant inhibitor. This computational strategy for discovering harmful mutations and screening for effective inhibitors of those mutations may soon contribute to the creation of tailored medicine.

## Materials and Methods

### Collection of data

The mutations and their combined information for the Cx43 Missense variant were retrieved from databases like COSMIC (https://cancer.sanger.ac.uk/cosmic), HGMD (http://www.hgmd.cf.ac.uk/ac/index.php), and literature survey. Sequence information of Cx43 in FASTA format was retrieved from Uniport KB (https://www.uniprot.org/).

### Pathogenicity analysis of missense variant

Calculation methods were used to understand the impact of variations on proteins which is vital for classifying and prioritizing pathogenic in neutral single-nucleotidevariations[15].

Meta-SNP (http://snps.biofold.org/meta-snp/) is a web-based server for many genome-related studies, which improves the ability to detect more heterogeneity of associations and investigate the consistency from different data sets and research populations. It integrates the best performance prediction algorithms to classify the pathogenicity of protein variants. In addition, the algorithm integrates with various other algorithms, including SNAP prediction, PhD SNP prediction, PANTHER prediction, and SIFT prediction. The predictor outputs the probability that the specified variant is associated with the disease. Here a score of > 0.5 establishes that a particular mutation induces the disease.

Functional impact analysis of the missense variant was done with the help of the Mutation Assessor server (http://mutationassessor.org/r3/). It is a network-dependent application that leverages disease-related Online Mendelian Inheritance in Man (OMIM) and polymorphism information to assess the effects of changes in a single-point amino acid change. The mutation assessor uses the Uniport protein sequence to generate its Multiple sequence alignment (MSA). It then splits based on the boundaries of the Uniport and Pfam domains to generate a 3D structure using a sorted product set and subfamily set. The segmented MSA was created to identify evolutionarily conserved locations that contribute to the specificity of protein function. Conservation scores are combined with specificity assessments to determine functional impact. As an outcome, mutants classified as "neutral" or "low" are not expected to affect protein function, whereas mutants classified as "medium" or "high" are functional and are expected to bring about changes.

### Structure stability analysis

Structure stability analysis helps determine whether a protein will be in a native folded conformation or a denatured state. It refers to physical stability (thermodynamic) and not chemical stability. Mutations in the protein frequently change the stability of the protein[16]. Here, the difference in free energy (ΔΔG) between the mutant (ΔGm) and the wild-type protein (ΔGw) is a measure of how a particular mutation affects the stability ofthe protein. A positive ΔΔG value shows a stabilizing mutation. We used different computational methods like DUET, MUpro, INPS-MD, i-Mutant 2.0, and Dyna Mut.

DUET (http://biosig.unimelb.edu.au/duet/stability) is a web server for integrated computer access to study missense mutations in proteins. It combines two

complementary approaches (mCSM and SDM) of consensus prediction obtained by blending results of particular methods in prediction optimized using SVM (Support Vector Machines). DUET improves the overall accuracy of the forecast compared to either technique by itself. By selectively combining the two methods, it far surpasses another integrated approach that combines the seven methods.

Mupro (http://mupro.proteomics.ics.uci.edu/) is a set of machine learning programs for predicting the effects of single-site amino acid mutations on protein stability. Two machine learning methods were developed, which are SVM and Neural Networks. An advantage of the method is that it does not require a tertiary structure to predict changes in protein stability.

INPS-MD (https://inpsmd.biocomp.unibo.it/inpsSuite/default/index3D) (Impact of Nonsynonymous mutations on Protein Stability Multi Dimension) is a web server designed to predict changes in protein stability duringa single point mutation. Currently, two versions of predictive variables are used. INPS prediction variable from the sequence: Prediction of the impact of nonsynonymous Single Nucleotide Polymorphisms (nsSNPs) on protein stability on protein stability sequence. INPS Predictor of protein 3D structure: Predicting the impact of asynchronous ns SNP for protein stability, starting with protein Structure.

I-Mutant2.0 (https://folding.biofold.org/cgi-bin/i-mutant2.0.cgi) is an SVM-based tool for automatically predicting changes in protein stability due to single-point mutations. These predictions are performed starting from the structure of the protein or, more importantly, the protein's sequence. IMutant2.0 is a classifier that predicts signs of changes in the stability of a protein upon mutation, which can be used as a regression estimator to predict the relevant $\Delta\Delta G$ values. The web server passes the protein array into its raw format.

Dyna Mut(http://biosig.unimelb.edu.au/dynamut/prediction) implements two well-established, normal-mode approaches to web servers that sample structures, analyze and visualize protein dynamics, and determine protein dynamics and stability due to vibrational entropy changes. It accommodates graph-based signatures with normal mode dynamics to achieve consensus predictions about the effects of mutations on protein stability. It also offers a comprehensive suite for protein motility, flexibility analysis, and visualization via a free, user-friendly web server[17].

**Predicted binding site**

COACH-D (https://yanglab.nankai.edu.cn/COACH-D/) is a method for accessing the meta server for predicting protein-ligand binding sites. It starts with a specific target protein structure and uses two comparative methods, TMSITE and SSITE, to generate a prediction of the complementary ligand-binding site. This method recognizes ligand binding templates in the functional database of BioLiP proteins by comparing binding-specific sub structures and sequence profiles. Initially, five separate ways are used to predict the ligand-binding pockets and residues. The template is then docked in the binding pocket. One of the significant improvements of COACH-D over COACH is that it uses Auto Dock Vina, an efficient molecular docking algorithm, to improve the ligand binding pose and make it physically and more realistic. The major conclusion is:Predicted 3D structural model submitted with a protein sequence, Top 5 protein-ligand binding pockets and binding residues in each pocket, top 5 protein-ligand complexes, submitted ligand docking structures, ligand docking from template structures, top 5 protein-ligand complex structures[18].

**Modelling native and variant protein**

I-TASSER (https://zhanglab.dcmb.med.umich.edu/I-TASSER/) (Iterative Threading Assembly Refinement) is a progressive way to deal with protein structure forecast and structure-based function annotation. First, structural templates in the PDB by a multi-threaded approach were identified using LOMETS full-length atomic models built by iterative template-based fragment assembly simulations. Next, the 3D model is re-threaded through the protein function database BioLiP to derive insight into the target function. It was recently ranked as the No.1 server for protein structure prediction in CASP7, CASP8, CASP9, CASP10, CASP11, CASP12, CASP13, and CASP14 experiments throughout society. It has also been evaluated with CASP9 for functional prediction. The server is under dynamic improvement, fully intent on giving the most exact protein design and capacity forecasts utilizing modern algorithms.

Loop refined was done using the HADDOCK server (https://wenmr.science.uu.nl/haddock2.4/refinement/1). High Ambiguity Driven Protein Docking) is an information-driven, flexible docking approach for the modelling of biomolecular complexes. HADDOCK differs from the abiniteo docking method in that it

encodes information at a protein interface identified or predicted in ambiguous interaction inhibition (AIR) to drive the docking process. It is also possible to define specific, clear distance limits(suchas MS cross-links),NMR residual dipole coupled pseudo-contact shifts, frozen EM maps, and many other experimental data supports. HADDOCK Proteins can deal with a massive class of displaying issues, including proteins, protein-nucleic acids, protein-ligand buildings, and multi-body (n>2) gatherings. HADDOCK is one of the flagship software for biomolecular research at the EU H2020 Bio excel center of excellence[19].

Structures were validated by the Ramachandran plot server (https://zlab.umassmed.edu/bu/rama/index.pl). This server displays Ramachandran plots against the background of whiplash probabilities, and the method server display color Ramachandran Plot. According to DSSP, blue means helix, red means strand, and green means turn-and-loop. The plotline shows the priority area. The outline surrounds the area where 90% of crosses of the same color are found. Lines inside show 50% area.

#### Conservative sequence analysis

ConSurf server (https://consurf.tau.ac.il/) is a bioinformatics tool for estimating the evolutionary storage of amino/nucleic acid positions of protein/DNA/RNA molecules according to phylogenetic relationships between homologous sequences. The extent to which the position of an amino acid (or nucleic acid) is evolutionarily conserved (*i.e.*, its rate of evolution) is highly dependent on the structural and functional significance. Therefore, analysis of position storage between members of the same family often clarifies the importance of each position to the structure or function of a protein (or nucleic acid). ConSurf estimates evolutionary rates by considering the similarities between amino acids (nucleic acids) that are reflected in alternative matrices according to the evolutionary relevance between proteins (DNA/RNA) and their homologs. One of the upsides of ConSurf over different techniques is that it precisely computes the pace of development utilizing either the exact Bayes strategy or the most extreme probability (ML) strategy[20].

#### Preparation of ligands

Thirty-six compounds were scrutinized by a literature survey based on the inhibitory effect on Cx43[4,5]. The information and SDF format of the 3D structure of the compounds were obtained from the PubChem database (https://pubchem.ncbi.nlm.nih.gov/). SDF formatted compounds were further converted to PDBQT format by Open Babel software which was used for docking[21].

#### Molecular docking

Molecular docking was performed by using the Autodock Vina software. Water from the native and L214P mutated proteins was removed, and polar hydrogen, solvation, and charges were added to the proteins. Affinity maps with grid points were fixed for the active binding sites of the proteins by using the Auto Grid program. A Lamarckian genetic algorithm was used to perform protein-ligand docking in Autodock vina. The results obtained from 10 different runs for each docking complex, among the highest binding energy complexes, were visualized by Pymol and Discovery studio software.

## Results

#### Metadata and disease-causing missense

A list of 249 missense variants for Cx43 was retrieved from public databases and literature review, followed by missense repetition removed and finalized to 219 missense variants. These missenses were then screened for pathogenicity analysis using a meta-SNP web-based server which includes PANTHER, PhD-SNP, SIFT, SNAP, and meta-SNP server (Fig. 1). As a result, among 219 missense, 52 missense variants were found to have deleterious in all the servers, which were taken to functional impact analysis (Table 1).

#### Function impact analysis of selected Cx43 mutations

The functional impact of the selected 52 missenses was examined using a mutation assessor server. As a result, 24 mutations were predicted to have a significant impact, and 22 missenses were shown to

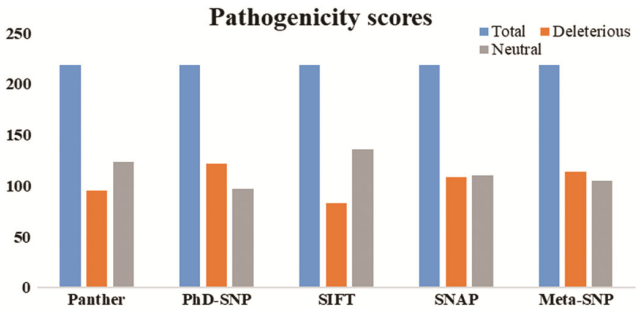


Fig. 1 — Deleterious and neutral mutation screening of Cx43 missense

Table 1 — Cx43 mutations were classified as deleterious or neutral using the meta-SNP server

| | | Panther | | PhD-SNP | | SIFT | | SNAP | | Meta-SNP | |
|---|---|---|---|---|---|---|---|---|---|---|---|
| Sl.no | Mutations (AA) | Disease | score | Disease | score | Disease | score | Disease | score | Disease | score |
| 1 | P363L | YES | 0.603 | NO | 0.233 | NO | 0.37 | NO | 0.465 | NO | 0.344 |
| 2 | S369N | NO | 0.437 | NO | 0.123 | NO | 0.56 | NO | 0.29 | NO | 0.145 |
| 3 | R370S | NO | 0.294 | NO | 0.12 | NO | 0.74 | NO | 0.315 | NO | 0.104 |
| 4 | R370H | NO | 0.229 | NO | 0.087 | NO | 0.12 | NO | 0.45 | NO | 0.07 |
| 5 | E381K | NO | 0.239 | NO | 0.047 | NO | 0.85 | NO | 0.19 | NO | 0.057 |
| 6 | W4C | YES | 0.829 | YES | 0.66 | YES | 0 | YES | 0.765 | YES | 0.747 |
| 7 | A6T | NO | 0.364 | NO | 0.079 | NO | 0.07 | NO | 0.145 | NO | 0.275 |
| 8 | K13N | NO | 0.459 | YES | 0.5 | NO | 0.27 | NO | 0.225 | NO | 0.446 |
| 9 | Y17C | YES | 0.774 | YES | 0.855 | YES | 0 | YES | 0.725 | YES | 0.811 |
| 10 | G21E | NO | 0.29 | YES | 0.683 | YES | 0 | YES | 0.645 | YES | 0.749 |
| 11 | W25R | YES | 0.639 | YES | 0.978 | YES | 0 | YES | 0.795 | YES | 0.91 |
| 12 | R33Q | YES | 0.997 | YES | 0.935 | YES | 0 | YES | 0.815 | YES | 0.952 |
| 13 | L37P | YES | 0.716 | YES | 0.962 | YES | 0 | YES | 0.61 | YES | 0.817 |
| 14 | S43T | NO | 0.318 | NO | 0.275 | NO | 0.25 | NO | 0.235 | NO | 0.458 |
| 15 | S43L | NO | 0.469 | YES | 0.626 | NO | 0.09 | NO | 0.405 | YES | 0.516 |
| 16 | Q49K | NO | 0.262 | YES | 0.721 | YES | 0.02 | YES | 0.665 | YES | 0.561 |
| 17 | R53G | NO | 0.277 | NO | 0.323 | NO | 0.06 | NO | 0.48 | NO | 0.469 |
| 18 | R53C | YES | 0.556 | NO | 0.494 | YES | 0.01 | YES | 0.56 | YES | 0.696 |
| 19 | R53H | NO | 0.284 | NO | 0.169 | YES | 0.05 | NO | 0.4 | NO | 0.302 |
| 20 | R53L | NO | 0.207 | NO | 0.337 | NO | 0.1 | NO | 0.425 | NO | 0.459 |
| 21 | G60C | YES | 0.999 | YES | 0.945 | YES | 0 | YES | 0.705 | YES | 0.921 |
| 22 | C61S | NO | 0.468 | YES | 0.946 | YES | 0.03 | YES | 0.64 | YES | 0.785 |
| 23 | K68N | NO | 0.405 | NO | 0.323 | NO | 0.59 | NO | 0.32 | NO | 0.466 |
| 24 | P71T | YES | 0.998 | YES | 0.952 | YES | 0 | YES | 0.755 | YES | 0.896 |
| 25 | R76C | YES | 0.812 | YES | 0.942 | YES | 0 | YES | 0.835 | YES | 0.924 |
| 26 | V79F | YES | 0.524 | YES | 0.9 | YES | 0.02 | YES | 0.59 | YES | 0.619 |
| 27 | F84C | YES | 0.783 | YES | 0.931 | YES | 0.04 | YES | 0.62 | YES | 0.749 |
| 28 | V85G | YES | 0.576 | YES | 0.952 | YES | 0 | YES | 0.745 | YES | 0.898 |
| 29 | P88L | YES | 0.641 | YES | 0.97 | YES | 0 | YES | 0.735 | YES | 0.877 |
| 30 | A94D | YES | 0.552 | YES | 0.851 | YES | 0.01 | YES | 0.6 | YES | 0.814 |
| 31 | A94V | NO | 0.408 | YES | 0.532 | NO | 0.26 | NO | 0.27 | NO | 0.455 |
| 32 | Y98S | YES | 0.576 | YES | 0.894 | YES | 0 | YES | 0.625 | YES | 0.77 |
| 33 | R101Q | NO | 0.478 | YES | 0.668 | NO | 0.13 | NO | 0.49 | YES | 0.529 |
| 34 | E103K | NO | 0.362 | YES | 0.706 | NO | 0.11 | YES | 0.54 | YES | 0.584 |
| 35 | E104D | NO | 0.276 | YES | 0.562 | YES | 0.03 | NO | 0.475 | YES | 0.52 |
| 36 | E110K | NO | 0.417 | NO | 0.219 | NO | 0.42 | NO | 0.49 | NO | 0.411 |
| 37 | E112K | NO | 0.417 | NO | 0.276 | NO | 0.69 | NO | 0.325 | NO | 0.443 |
| 38 | K114N | NO | 0.439 | NO | 0.212 | NO | 0.49 | NO | 0.34 | NO | 0.37 |
| 39 | A116V | NO | 0.054 | NO | 0.136 | NO | 0.28 | NO | 0.415 | NO | 0.302 |
| 40 | G120A | NO | 0.423 | NO | 0.39 | NO | 0.5 | NO | 0.46 | NO | 0.45 |
| 41 | V123A | NO | 0.34 | NO | 0.141 | NO | 0.55 | NO | 0.38 | NO | 0.168 |
| 42 | M125I | NO | 0.126 | NO | 0.16 | NO | 0.13 | NO | 0.385 | NO | 0.228 |
| 43 | L127W | YES | 0.831 | YES | 0.505 | NO | 0.13 | NO | 0.405 | YES | 0..552 |
| 44 | L127F | NO | 0.45 | NO | 0.254 | NO | 0.48 | NO | 0.205 | NO | 0.429 |
| 45 | Q129E | NO | 0.159 | NO | 0.19 | NO | 1 | NO | 0.185 | NO | 0.301 |
| 46 | K133N | NO | 0.431 | NO | 0.39 | NO | 0.37 | NO | 0.205 | NO | 0.463 |
| 47 | G138C | YES | 0.805 | NO | 0.418 | NO | 0.05 | NO | 0.48 | YES | 0.625 |
| 48 | E141K | NO | 0.411 | YES | 0.545 | NO | 0.76 | NO | 0.28 | NO | 0.459 |
| 49 | V145L | NO | 0.223 | NO | 0.361 | NO | 0.35 | NO | 0.175 | NO | 0.433 |
| 50 | G149E | YES | 0.996 | YES | 0.872 | NO | 0.12 | YES | 0.59 | YES | 0.866 |

(*Contd.*)

Table 1 — Cx43 mutations were classified as deleterious or neutral using the meta-SNP server (*Contd*.)

| | | Panther | | PhD-SNP | | SIFT | | SNAP | | Meta-SNP | |
|---|---|---|---|---|---|---|---|---|---|---|---|
| Sl.no | Mutations (AA) | Disease | score | Disease | score | Disease | score | Disease | score | Disease | score |
| 101 | S306N | NO | 0.126 | NO | 0.317 | NO | 0.31 | NO | 0.32 | NO | 0.3 |
| 102 | S314R | NO | 0.494 | NO | 0.387 | NO | 0.41 | NO | 0.325 | NO | 0.291 |
| 103 | Q317R | NO | 0.324 | NO | 0.299 | NO | 0.5 | NO | 0.375 | NO | 0.293 |
| 104 | R319Q | NO | 0.423 | NO | 0.332 | NO | 0.29 | NO | 0.475 | NO | 0.315 |
| 105 | A323V | NO | 0.302 | NO | 0.195 | NO | 0.3 | NO | 0.46 | NO | 0.244 |
| 106 | G324E | YES | 0.583 | YES | 0.58 | NO | 1 | NO | 0.41 | NO | 0.448 |
| 107 | S328P | YES | 0.525 | YES | 0.62 | NO | 0.29 | NO | 0.2 | NO | 0.445 |
| 108 | S330F | YES | 0.594 | YES | 0.572 | NO | 0.7 | NO | 0.34 | NO | 0.462 |
| 109 | A332T | NO | 0.347 | NO | 0.269 | NO | 0.58 | NO | 0.325 | NO | 0.265 |
| 110 | D336V | YES | 0.633 | NO | 0.368 | NO | 0.28 | NO | 0.48 | NO | 0.45 |
| 111 | D340N | NO | 0.225 | NO | 0.456 | NO | 0.35 | NO | 0.26 | NO | 0.342 |
| 112 | D340Y | YES | 0.619 | YES | 0.673 | NO | 1 | NO | 0.25 | YES | 0.532 |
| 113 | Q342R | NO | 0.107 | NO | 0.318 | NO | 0.33 | YES | 0.505 | NO | 0.294 |
| 114 | N343H | NO | 0.374 | NO | 0.19 | NO | 0.15 | NO | 0.435 | NO | 0.246 |
| 115 | K345R | NO | 0.242 | NO | 0.108 | NO | 0.49 | NO | 0.215 | NO | 0.088 |
| 116 | L347P | YES | 0.642 | YES | 0.653 | NO | 0.27 | NO | 0.435 | NO | 0.455 |
| 117 | A348T | NO | 0.092 | NO | 0.127 | NO | 0.59 | NO | 0.23 | NO | 0.11 |
| 118 | G350E | YES | 0.574 | NO | 0.44 | NO | 1 | NO | 0.315 | NO | 0.458 |
| 119 | L356R | YES | 0.623 | YES | 0.712 | NO | 0.52 | NO | 0.3 | YES | 0.539 |
| 120 | V359L | NO | 0.111 | NO | 0.073 | NO | 0.74 | NO | 0.32 | NO | 0.065 |
| 121 | D360E | NO | 0.274 | NO | 0.302 | NO | 1 | NO | 0.225 | NO | 0.256 |
| 122 | T19A | NO | 0.142 | YES | 0.853 | YES | 0 | YES | 0.77 | YES | 0.786 |
| 123 | V28I | NO | 0.166 | NO | 0.498 | NO | 0.24 | YES | 0.51 | NO | 0.429 |
| 124 | A44V | NO | 0.367 | NO | 0.08 | NO | 1 | NO | 0.215 | NO | 0.266 |
| 125 | E227D | YES | 0.993 | YES | 0.883 | YES | 0.04 | YES | 0.65 | YES | 0.576 |
| 126 | P283L | YES | 0.637 | YES | 0.564 | NO | 0.05 | YES | 0.645 | YES | 0.51 |
| 127 | T290D | YES | 0.515 | NO | 0.429 | NO | 0.66 | YES | 0.56 | NO | 0.372 |
| 128 | Y17S | YES | 0.531 | YES | 0.792 | YES | 0 | YES | 0.66 | YES | 0.76 |
| 129 | G143S | NO | 0.455 | YES | 0.626 | NO | 0.58 | NO | 0.405 | NO | 0.477 |
| 130 | G138I | YES | 0.785 | NO | 0.294 | NO | 0.2 | NO | 0.37 | NO | 0.464 |
| 131 | S18P | YES | 0.994 | YES | 0.913 | YES | 0 | YES | 0.805 | YES | 0.92 |
| 132 | G21R | NO | 0.351 | YES | 0.741 | YES | 0 | YES | 0.655 | YES | 0.758 |
| 133 | G22E | YES | 0.565 | YES | 0.962 | YES | 0 | YES | 0.845 | YES | 0.933 |
| 134 | G60S | YES | 0.997 | YES | 0.913 | YES | 0 | YES | 0.685 | YES | 0.879 |
| 135 | G138R | YES | 0.716 | NO | 0.435 | NO | 0.53 | NO | 0.435 | YES | 0.566 |
| 136 | V96M | NO | 0.451 | YES | 0.73 | YES | 0.03 | YES | 0.645 | YES | 0.682 |
| 137 | I31M | NO | 0.407 | YES | 0.814 | YES | 0 | YES | 0.66 | YES | 0.681 |
| 138 | G8V | NO | 0.348 | YES | 0.628 | YES | 0.04 | YES | 0.645 | NO | 0.454 |
| 139 | G2V | YES | 0.59 | NO | 0.447 | YES | 0 | YES | 0.62 | YES | 0.597 |
| 140 | D3N | NO | 0.257 | NO | 0.113 | NO | 0.15 | NO | 0.25 | NO | 0.231 |
| 141 | S5C | YES | 0.648 | NO | 0.335 | YES | 0 | NO | 0.465 | YES | 0.596 |
| 142 | L7V | NO | 0.3 | NO | 0.483 | YES | 0.01 | YES | 0.77 | YES | 0.578 |
| 143 | L11I | NO | 0.274 | YES | 0.518 | YES | 0.04 | YES | 0.645 | NO | 0.454 |
| 144 | L11P | YES | 0.743 | YES | 0.907 | YES | 0 | YES | 0.775 | YES | 0.818 |
| 145 | L11F | NO | 0.426 | YES | 0.734 | YES | 0.01 | YES | 0.675 | YES | 0.648 |
| 146 | G22R | YES | 0.652 | YES | 0.962 | YES | 0.02 | YES | 0.84 | YES | 0.93 |
| 147 | K23T | NO | 0.437 | YES | 0.893 | YES | 0 | YES | 0.735 | YES | 0.807 |
| 148 | V24A | NO | 0.327 | YES | 0.765 | YES | 0 | YES | 0.64 | YES | 0.706 |
| 149 | W25C | YES | 0.806 | YES | 0.974 | YES | 0 | YES | 0.775 | YES | 0.892 |
| 150 | S27P | NO | 0.442 | YES | 0.955 | YES | 0.04 | YES | 0.595 | YES | 0.623 |

(*Contd*.)

Table 1 — Cx43 mutations were classified as deleterious or neutral using the meta-SNP server (*Contd.*)

| | | Panther | | PhD-SNP | | SIFT | | SNAP | | Meta-SNP | |
|---|---|---|---|---|---|---|---|---|---|---|---|
| Sl.no | Mutations (AA) | Disease | score | Disease | score | Disease | score | Disease | score | Disease | score |
| 151 | A40V | NO | 0.367 | YES | 0.637 | NO | 0.09 | YES | 0.585 | YES | 0.501 |
| 152 | V41L | NO | 0.177 | NO | 0.437 | YES | 0.02 | YES | 0.51 | NO | 0.497 |
| 153 | E42L | YES | 0.527 | YES | 0.793 | YES | 0.01 | YES | 0.66 | YES | 0.709 |
| 154 | E42Q | NO | 0.406 | YES | 0.687 | YES | 0.03 | YES | 0.545 | YES | 0.528 |
| 155 | D47H | YES | 0.998 | YES | 0.878 | YES | 0 | YES | 0.75 | YES | 0.889 |
| 156 | E48L | YES | 0.527 | YES | 0.818 | YES | 0 | YES | 0.715 | YES | 0.744 |
| 157 | Q49L | NO | 0.421 | YES | 0.781 | YES | 0 | YES | 0.655 | YES | 0.661 |
| 158 | Q49P | YES | 0.56 | YES | 0.88 | YES | 0 | YES | 0.655 | YES | 0.761 |
| 159 | Q49E | NO | 0.299 | YES | 0.666 | YES | 0.02 | YES | 0.66 | YES | 0.605 |
| 160 | N55D | NO | 0.344 | YES | 0.615 | NO | 0.15 | YES | 0.62 | NO | 0.441 |
| 161 | Q58H | YES | 0.588 | YES | 0.845 | YES | 0 | YES | 0.71 | YES | 0.779 |
| 162 | P59H | YES | 0.999 | YES | 0.893 | YES | 0 | YES | 0.78 | YES | 0.937 |
| 163 | P59A | YES | 0.997 | YES | 0.796 | YES | 0.02 | YES | 0.7 | YES | 0.851 |
| 164 | S69Y | YES | 0.626 | YES | 0.706 | NO | 1 | NO | 0.28 | YES | 0.578 |
| 165 | H74L | YES | 0.522 | YES | 0.908 | NO | 0.13 | YES | 0.615 | YES | 0.598 |
| 166 | R76S | NO | 0.491 | YES | 0.926 | YES | 0 | YES | 0.78 | YES | 0.817 |
| 167 | R76H | YES | 0.621 | YES | 0.932 | YES | 0.02 | YES | 0.82 | YES | 0.848 |
| 168 | V85M | YES | 0.506 | YES | 0.882 | YES | 0.01 | YES | 0.73 | YES | 0.779 |
| 169 | S86Y | YES | 0.683 | YES | 0.954 | YES | 0 | YES | 0.725 | YES | 0.886 |
| 170 | L90V | NO | 0.304 | YES | 0.718 | NO | 0.13 | NO | 0.485 | YES | 0.55 |
| 171 | H95R | NO | 0.468 | YES | 0.909 | YES | 0 | YES | 0.79 | YES | 0.836 |
| 172 | V96E | YES | 0.571 | YES | 0.921 | YES | 0.01 | YES | 0.8 | YES | 0.856 |
| 173 | V96A | NO | 0.312 | NO | 0.322 | NO | 0.83 | NO | 0.42 | NO | 0.45 |
| 174 | Y98C | YES | 0.802 | YES | 0.904 | YES | 0 | YES | 0.67 | YES | 0.791 |
| 175 | R101L | YES | 0.564 | YES | 0.831 | NO | 0.07 | NO | 0.47 | YES | 0.704 |
| 176 | K102N | NO | 0.439 | NO | 0.42 | NO | 0.36 | NO | 0.47 | NO | 0.475 |
| 177 | L106P | YES | 0.768 | YES | 0.712 | NO | 0.32 | NO | 0.46 | YES | 0.562 |
| 178 | L106R | YES | 0.683 | NO | 0.383 | NO | 1 | NO | 0.27 | YES | 0.576 |
| 179 | E110D | NO | 0.32 | NO | 0.206 | NO | 0.17 | YES | 0.525 | NO | 0.387 |
| 180 | L113P | YES | 0.768 | YES | 0.638 | NO | 0.33 | YES | 0.62 | YES | 0.596 |
| 181 | I130T | NO | 0.432 | NO | 0.402 | NO | 0.56 | NO | 0.475 | NO | 0.439 |
| 182 | K134N | NO | 0.431 | NO | 0.477 | NO | 0.51 | NO | 0.415 | NO | 0.474 |
| 183 | K134E | NO | 0.347 | NO | 0.496 | NO | 1 | NO | 0.37 | NO | 0.46 |
| 184 | G138S | YES | 0.517 | NO | 0.128 | NO | 0.73 | NO | 0.23 | NO | 0.159 |
| 185 | G138D | YES | 0.643 | NO | 0.478 | NO | 0.62 | NO | 0.49 | YES | 0.546 |
| 187 | G143D | YES | 0.582 | YES | 0.875 | NO | 0.48 | YES | 0.66 | YES | 0.714 |
| 188 | K144E | NO | 0.347 | YES | 0.813 | NO | 0.05 | YES | 0.58 | YES | 0.6 |
| 189 | V145G | YES | 0.545 | YES | 0.651 | NO | 0.38 | NO | 0.275 | NO | 0.472 |
| 190 | M147T | NO | 0.473 | YES | 0.5 | NO | 0.23 | YES | 0.55 | YES | 0.643 |
| 191 | R148Q | NO | 0.222 | YES | 0.608 | NO | 0.23 | YES | 0.615 | NO | 0.478 |
| 192 | R148G | NO | 0.413 | YES | 0.824 | NO | 0.14 | YES | 0.72 | YES | 0.765 |
| 193 | R153Q | NO | 0.416 | YES | 0.651 | NO | 0.32 | NO | 0.465 | YES | 0.513 |
| 194 | T154N | YES | 0.526 | YES | 0.898 | YES | 0.02 | YES | 0.715 | YES | 0.798 |
| 195 | T154A | NO | 0.292 | YES | 0.687 | NO | 0.14 | YES | 0.51 | YES | 0.531 |
| 196 | P193L | YES | 0.686 | YES | 0.875 | YES | 0.04 | YES | 0.635 | YES | 0.637 |
| 197 | H194P | YES | 0.657 | YES | 0.868 | YES | 0.01 | YES | 0.705 | YES | 0.806 |
| 198 | S201Y | YES | 0.719 | YES | 0.914 | YES | 0 | YES | 0.78 | YES | 0.829 |
| 199 | S201F | YES | 0.701 | YES | 0.899 | YES | 0 | YES | 0.785 | YES | 0.831 |
| 200 | R202H | YES | 0.66 | YES | 0.862 | YES | 0.01 | YES | 0.755 | YES | 0.672 |
| 201 | K206R | YES | 0.992 | YES | 0.879 | YES | 0 | YES | 0.69 | YES | 0.858 |

(*Contd.*)

Table 1 — Cx43 mutations were classified as deleterious or neutral using the meta-SNP server (*Contd*.)

| | | Panther | | PhD-SNP | | SIFT | | SNAP | | Meta-SNP | |
|---|---|---|---|---|---|---|---|---|---|---|---|
| Sl.no | Mutations (AA) | Disease | score | Disease | score | Disease | score | Disease | score | Disease | score |
| 202 | V216L | NO | 0.272 | YES | 0.778 | YES | 0.03 | YES | 0.66 | YES | 0.605 |
| 203 | S220Y | YES | 0.719 | YES | 0.896 | YES | 0.01 | YES | 0.685 | YES | 0.779 |
| 204 | R239Q | NO | 0.317 | NO | 0.457 | NO | 0.36 | YES | 0.58 | NO | 0.451 |
| 205 | R239W | YES | 0.809 | YES | 0.701 | NO | 0.18 | YES | 0.6 | YES | 0.733 |
| 206 | S251T | NO | 0.122 | NO | 0.084 | NO | 0.6 | NO | 0.38 | NO | 0.132 |
| 207 | A253P | NO | 0.069 | NO | 0.389 | NO | 0.28 | NO | 0.36 | NO | 0.348 |
| 208 | A253V | NO | 0.161 | NO | 0.207 | NO | 0.34 | YES | 0.515 | NO | 0.272 |
| 209 | G261W | YES | 0.745 | YES | 0.661 | YES | 0.02 | YES | 0.64 | YES | 0.711 |
| 210 | S272P | YES | 0.545 | YES | 0.72 | NO | 0.5 | NO | 0.25 | YES | 0.503 |
| 211 | A276P | YES | 0.568 | NO | 0.482 | NO | 0.29 | NO | 0.265 | NO | 0.484 |
| 212 | T290N | NO | 0.497 | NO | 0.391 | NO | 0.74 | NO | 0.335 | NO | 0.311 |
| 213 | A323G | NO | 0.274 | NO | 0.14 | NO | 0.4 | NO | 0.395 | NO | 0.13 |
| 214 | T326I | NO | 0.429 | NO | 0.278 | NO | 0.26 | NO | 0.22 | NO | 0.338 |
| 215 | E352G | NO | 0.441 | NO | 0.495 | NO | 0.3 | YES | 0.61 | YES | 0.682 |
| 216 | R362Q | NO | 0.416 | YES | 0.567 | NO | 0.59 | YES | 0.565 | YES | 0.636 |
| 217 | S364P | NO | 0.213 | NO | 0.232 | NO | 0.24 | NO | 0.41 | NO | 0.264 |
| 218 | S365N | NO | 0.437 | NO | 0.377 | NO | 0.33 | NO | 0.36 | NO | 0.369 |
| 219 | R376Q | NO | 0.416 | YES | 0.507 | NO | 0.51 | YES | 0.595 | YES | 0.611 |

Table 2 — Functional impact of selected missense in Cx43 protein

| Sl.no | Mutations | FI score | VC score | VS score | Functional impact | Sl.no | Mutations | FI score | VC score | VS score | Functional impact |
|---|---|---|---|---|---|---|---|---|---|---|---|
| 1 | W4C | 3.81 | 5.14 | 2.48 | high | 27 | E205K | 4.04 | 5.68 | 2.4 | high |
| 2 | L11F | 3.21 | 3.94 | 2.48 | medium | 28 | D259Y | 1.245 | 1.39 | 1.1 | low |
| 3 | Y17C | 2.35 | 4.01 | 0.69 | medium | 29 | E227D | 2.63 | 2.86 | 2.4 | medium |
| 4 | G22E | 3.83 | 5.18 | 2.48 | high | 30 | Y17S | 1.655 | 2.62 | 0.69 | low |
| 5 | W25R | 3.815 | 5.15 | 2.48 | high | 31 | S18P | 3.805 | 5.13 | 2.48 | high |
| 6 | R33Q | 3.84 | 5.2 | 2.48 | high | 32 | G60S | 3.84 | 5.2 | 2.48 | high |
| 7 | L37P | 3.51 | 4.62 | 2.4 | high | 33 | L11P | 3.76 | 5.04 | 2.48 | high |
| 8 | P71T | 3.435 | 4.47 | 2.4 | medium | 34 | G22R | 3.83 | 5.18 | 2.48 | high |
| 9 | G60C | 3.84 | 5.2 | 2.48 | high | 35 | W25C | 3.47 | 4.46 | 2.48 | medium |
| 10 | R76C | 3.785 | 5.17 | 2.4 | high | 36 | E42L | Neutral | Neutral | Neutral | Neutral |
| 11 | R76H | 2.885 | 4.07 | 1.7 | medium | 37 | D47H | 3.48 | 4.48 | 2.48 | medium |
| 12 | V79F | 1.955 | 2.81 | 1.1 | medium | 38 | E48L | Neutral | Neutral | Neutral | Neutral |
| 13 | F84C | 2.725 | 3.84 | 1.61 | medium | 39 | Q49P | 3.65 | 5 | 2.3 | high |
| 14 | V85M | 3.61 | 5.02 | 2.2 | high | 40 | Q58H | 3.64 | 5.08 | 2.2 | high |
| 15 | V85G | 3.61 | 5.02 | 2.2 | high | 41 | P59H | 3.47 | 4.46 | 2.48 | medium |
| 16 | P88L | 3.835 | 5.19 | 2.48 | high | 42 | P59A | 3.815 | 5.15 | 2.48 | high |
| 17 | A94D | 1.495 | 2.3 | 0.69 | low | 43 | S86Y | 3.38 | 4.68 | 2.08 | medium |
| 18 | Y98S | 2.51 | 4.33 | 0.69 | medium | 44 | V96E | 3.48 | 4.66 | 2.3 | medium |
| 19 | T154N | 3.005 | 3.71 | 2.3 | medium | 45 | Y98C | 2.51 | 4.33 | 0.69 | medium |
| 20 | Y177C | 3.95 | 5.5 | 2.4 | high | 46 | P193L | 2.805 | 3.21 | 2.4 | medium |
| 21 | G178E | 3.97 | 5.54 | 2.4 | high | 47 | H194P | 3.385 | 4.47 | 2.3 | medium |
| 22 | H194L | 2.835 | 3.37 | 2.3 | medium | 48 | S201Y | 3.985 | 5.57 | 2.4 | high |
| 23 | R202H | 3.215 | 4.03 | 2.4 | medium | 49 | S201F | 3.985 | 5.57 | 2.4 | high |
| 24 | T204K | 2.925 | 3.45 | 2.4 | medium | 50 | K206R | 4.045 | 5.69 | 2.4 | high |
| 25 | T204M | 2.815 | 3.23 | 2.4 | medium | 51 | S220Y | 3.67 | 4.94 | 2.4 | high |
| 26 | L214P | 3.405 | 4.51 | 2.3 | medium | 52 | G261W | 1.59 | 1.79 | 1.39 | low |

have a medium impact on protein structure and functionality, which was calculated based on FI, VC, and VS scores. Furthermore, four mutations were found to have a low impact,and two mutations were predicted to have no impact on Cx43 protein functionality, respectively (Fig. 2 and Table 2). Thus, among 52 mutations,the functional impacts, including high and medium of 46 mutations, were taken to further analysis.

**Stability analysis of Selected Cx43 mutation**

From the mutation functional impact analysis, 46 mutations in the Cx43 protein were predicted to have a high and medium impact on protein functions which

was selected for stability analysis. The selected Cx43 mutant stability was analyzed using ΔΔG analysis-based servers such as DUET, Mupro, INPS-MD, I-Mutant2.0, and Dyna Mut (Table 3). As a result, the stability analysis servers, including mCSM, SDM, DUET, Mupro, INPS-MD, I MUTANT, I Stabilizing, ENCOM, and Dyna MUT predicted destabilizing mutations as 40, 30, 38, 42, 25, 39, 37, 25 and 22 respectively (Fig. 3). From the stability prediction, eight mutations (R76H, V79F, F84C, V85G, Y177C, L214P, G60S, and L11P) are commonly destabilizing in individual servers.

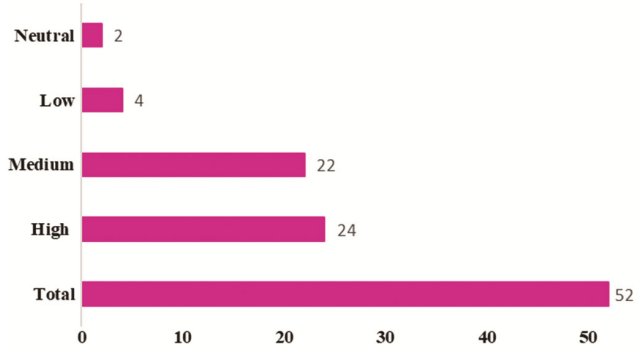


Fig. 2 — Functional impact prediction of Cx43 protein mutations

**Binding pocket prediction**

Ligand binding site prediction is important for protein regulation. Thus, modelled Cx43 native protein was subjected to predict binding pockets using the COACH-D server. COACH-D result analysis revealed native Cx43 shown to bind with ligands (FE, ZN, 0F1 and PTY) via 22 residues namely, ARG33, LEU37, VAL41, CYS54, CYS61, HIS74, ILE82, VAL166, PHE169, LEU170, GLN173, CYS187, CYS192, CYS198, ILE210, MET213, LEU214, SER217, LEU218, SER220, LEU221 and ALA222 which was considered for binding sites in native and mutant Cx43.

Of the selected eight mutations from stability analysis, a mutation cc was screened to have played a part in binding pockets. Thus, a mutation L214P was then selected for conservative structural analysis.

Table 3 — Stability analysis of Cx43 selected missenses

| | | DUET | | | | | | Mupro | | INPS–MD | | I MUTANT 2.0 SEQ | | Dyna Mut | | | | | |
|---|---|---|---|---|---|---|---|---|---|---|---|---|---|---|---|---|---|---|---|
| | | mCSM | | SDM | | DUET | | Mupro | | INPS–MD | | I MUTANT 2.0 SEQ | | I Stabilizing | | ENCOM | | Dyna Mut | |
| Sl. no | Mutations | ΔΔG | Stability | ΔΔG | Stability | ΔΔG | Stability | ΔΔG | Stability | ΔΔG | Stability | ΔΔG | Stability | ΔΔG | Stability | ΔΔG | Stability | ΔΔG | Stability |
| 1 | W4C | 0.254 | Stabilizing | –0.15 | Destabilizing | 0.39 | Stabilizing | –0.153 | Destabilizing | –1.56725 | Destabilizing | –1.55 | Destabilizing | 0.643 | Stabilizing | 0.002 | Stabilizing | 0.447 | Stabilizing |
| 2 | L11F | –0.77 | Destabilizing | –0.69 | Destabilizing | –0.844 | Destabilizing | –1.213 | Destabilizing | –1.1666655 | Destabilizing | –1 | Destabilizing | 0.91 | Destabilizing | 0.379 | Stabilizing | 0.556 | Stabilizing |
| 3 | Y17C | –0.46 | Destabilizing | –0.07 | Destabilizing | –0.29 | Destabilizing | –0.556 | Destabilizing | –1.496945 | Destabilizing | –0.82 | Stabilizing | 0.55 | Destabilizing | –0.699 | Destabilizing | –0.546 | Destabilizing |
| 4 | G22E | –2.031 | Destabilizing | 0.22 | Stabilizing | –1.592 | Destabilizing | –0.677 | Destabilizing | –0.7547255 | Stabilizing | –1.02 | Destabilizing | 0.83 | Destabilizing | 0.673 | Stabilizing | 0.213 | Stabilizing |
| 5 | W25R | –0.932 | Destabilizing | 0.32 | Stabilizing | –0.677 | Destabilizing | –0.784 | Destabilizing | –1.2714685 | Destabilizing | –1.49 | Destabilizing | 0.87 | Destabilizing | –0.286 | Destabilizing | –0.759 | Destabilizing |
| 6 | R33Q | –1.015 | Destabilizing | –1.97 | Destabilizing | –1.288 | Destabilizing | –0.799 | Destabilizing | –1.47021 | Destabilizing | –0.51 | Destabilizing | 0.741 | Destabilizing | –0.274 | Destabilizing | –1.494 | Destabilizing |
| 7 | L37P | –0.992 | Destabilizing | –4.41 | Destabilizing | –1.669 | Destabilizing | –2.02 | Destabilizing | –3.246535 | Destabilizing | –1.78 | Destabilizing | 0.798 | Destabilizing | –0.519 | Destabilizing | –0.962 | Destabilizing |
| 8 | P71T | –1.078 | Destabilizing | 0.16 | Stabilizing | –0.704 | Destabilizing | –1.311 | Destabilizing | –1.0029515 | Destabilizing | –1.56 | Destabilizing | 0.799 | Destabilizing | 0.284 | Stabilizing | 0.743 | Stabilizing |
| 9 | G60C | –0.682 | Destabilizing | –2.37 | Destabilizing | –1.054 | Destabilizing | 0.064 | Stabilizing | –1.683805 | Destabilizing | –1.15 | Destabilizing | 0.53 | Destabilizing | –0.085 | Destabilizing | –1.339 | Destabilizing |
| 10 | R76C | –0.995 | Destabilizing | –0.12 | Destabilizing | –0.827 | Destabilizing | –0.963 | Destabilizing | –0.2137374 | Stabilizing | –1.12 | Destabilizing | 0.833 | Destabilizing | –0.568 | Destabilizing | –0.329 | Destabilizing |
| 11 | R76H | –1.506 | Destabilizing | –0.56 | Destabilizing | –1.559 | Destabilizing | –1.285 | Destabilizing | –0.795757 | Destabilizing | –1.74 | Destabilizing | 0.845 | Destabilizing | –0.002 | Destabilizing | –0.222 | Destabilizing |
| 12 | V79F | –0.62 | Destabilizing | –0.41 | Destabilizing | –0.611 | Destabilizing | –1.201 | Destabilizing | –1.22595 | Destabilizing | –1.39 | Destabilizing | 0.82 | Destabilizing | –0.001 | Destabilizing | –0.261 | Destabilizing |
| 13 | F84C | –1.444 | Destabilizing | –0.2 | Destabilizing | –1.285 | Destabilizing | –1.399 | Destabilizing | –2.00914 | Destabilizing | –1.97 | Destabilizing | 0.66 | Destabilizing | –2.445 | Destabilizing | –1.137 | Destabilizing |
| 14 | V85M | –0.654 | Destabilizing | –0.63 | Destabilizing | –0.59 | Destabilizing | –0.898 | Destabilizing | –1.330545 | Destabilizing | –1.67 | Destabilizing | 0.73 | Destabilizing | 0.206 | Stabilizing | –0.056 | Destabilizing |
| 15 | V85G | –2.703 | Destabilizing | –2.37 | Destabilizing | –3.095 | Destabilizing | –2.23 | Destabilizing | –3.778675 | Destabilizing | –3.04 | Destabilizing | 0.83 | Destabilizing | –0.887 | Destabilizing | –2.258 | Destabilizing |
| 16 | P88L | 0.012 | Stabilizing | 2.12 | Stabilizing | 0.838 | Stabilizing | 0.36 | Stabilizing | –0.1627065 | Stabilizing | –0.86 | Destabilizing | 0.56 | Destabilizing | 0.321 | Stabilizing | 1.439 | Stabilizing |
| 17 | Y98S | –1.096 | Destabilizing | –0.54 | Destabilizing | –0.902 | Destabilizing | –1.147 | Destabilizing | –1.290914 | Destabilizing | –1.51 | Destabilizing | 0.74 | Destabilizing | 0.042 | Stabilizing | 0.412 | Stabilizing |
| 18 | T154N | –1.13 | Destabilizing | –0.15 | Destabilizing | –0.847 | Destabilizing | –1.141 | Destabilizing | –1.261667 | Destabilizing | –1.33 | Destabilizing | 0.76 | Destabilizing | –0.25 | Destabilizing | 0.572 | Stabilizing |
| 19 | Y177C | –1.423 | Destabilizing | –0.87 | Destabilizing | –1.336 | Destabilizing | –1.443 | Destabilizing | –1.922375 | Destabilizing | –1.26 | Destabilizing | 0.81 | Destabilizing | –1.43 | Destabilizing | –0.921 | Destabilizing |
| 20 | G178E | 0.098 | Stabilizing | –3.86 | Destabilizing | –0.407 | Destabilizing | –0.524 | Destabilizing | –1.0358325 | Destabilizing | –0.71 | Destabilizing | 0.76 | Destabilizing | –0.061 | Destabilizing | –1.608 | Destabilizing |
| 21 | H194L | 1.002 | Stabilizing | 0.21 | Stabilizing | 0.958 | Stabilizing | 0.235 | Stabilizing | –0.206911 | Stabilizing | 0.6 | Stabilizing | 0.7 | Stabilizing | –0.084 | Destabilizing | 0.359 | Stabilizing |
| 22 | R202H | –1.236 | Destabilizing | 0.5 | Stabilizing | –1.092 | Destabilizing | –1.162 | Destabilizing | –0.8287845 | Destabilizing | –1.48 | Destabilizing | 0.73 | Destabilizing | –0.114 | Destabilizing | –0.362 | Destabilizing |
| 23 | T204K | –0.521 | Destabilizing | 0.9 | Stabilizing | 0.107 | Stabilizing | –0.918 | Destabilizing | –0.5708325 | Stabilizing | –1.12 | Destabilizing | 0.64 | Stabilizing | –0.081 | Destabilizing | 0.041 | Stabilizing |
| 24 | T204M | 0.116 | Stabilizing | 0.62 | Stabilizing | 0.453 | Stabilizing | –0.193 | Destabilizing | –0.4244125 | Stabilizing | 0.02 | Destabilizing | 0.67 | Stabilizing | –0.073 | Destabilizing | 0.3 | Stabilizing |
| 25 | L214P | –1.075 | Destabilizing | –3.14 | Destabilizing | –1.508 | Destabilizing | –2.303 | Destabilizing | –3.150245 | Destabilizing | –1.47 | Destabilizing | 0.83 | Destabilizing | –0.66 | Destabilizing | –1.133 | Destabilizing |
| 26 | E205K | –0.457 | Destabilizing | –1 | Destabilizing | –0.282 | Destabilizing | –1.634 | Destabilizing | –0.4850575 | Stabilizing | –0.68 | Destabilizing | 0.81 | Destabilizing | 0.026 | Stabilizing | –0.302 | Destabilizing |
| 27 | E227D | –1.289 | Destabilizing | –1.99 | Destabilizing | –1.477 | Destabilizing | –0.869 | Destabilizing | –1.095409 | Destabilizing | –0.19 | Destabilizing | 0.605 | Stabilizing | –0.477 | Destabilizing | –1.291 | Destabilizing |
| 28 | S18P | –0.521 | Destabilizing | –0.45 | Destabilizing | –0.415 | Destabilizing | –1.236 | Destabilizing | –0.9889335 | Stabilizing | –0.01 | Stabilizing | 0.81 | Stabilizing | 0.013 | Stabilizing | 0.349 | Stabilizing |
| 29 | G60S | –0.656 | Destabilizing | –3.84 | Destabilizing | –1.102 | Destabilizing | –0.242 | Destabilizing | –1.0329635 | Destabilizing | –1.42 | Destabilizing | 0.53 | Destabilizing | –0.082 | Destabilizing | –1.37 | Destabilizing |
| 30 | L11P | –0.728 | Destabilizing | –2.63 | Destabilizing | –1.015 | Destabilizing | –1.95 | Destabilizing | –2.72524 | Destabilizing | –1.54 | Destabilizing | 0.909 | Destabilizing | –0.427 | Destabilizing | –0.531 | Destabilizing |
| 31 | G22R | –0.935 | Destabilizing | –0.46 | Destabilizing | –0.673 | Destabilizing | –0.704 | Destabilizing | –0.365542 | Stabilizing | –1.04 | Destabilizing | 0.79 | Destabilizing | 1.346 | Stabilizing | 1.374 | Stabilizing |

(*Contd.*)

Table 3 — Stability analysis of Cx43 selected missenses (*Contd.*)

| | | | | DUET | | | | Mupro | | INPS–MD | | I MUTANT 2.0 SEQ | | | | Dyna Mut | | | |
|---|---|---|---|---|---|---|---|---|---|---|---|---|---|---|---|---|---|---|---|
| | | mCSM | | SDM | | DUET | | Mupro | | INPS–MD | | I MUTANT 2.0 SEQ | | I Stabilizing | | ENCOM | | Dyna Mut | |
| Sl. no | Mutations | ΔΔG | Stability | ΔΔG | Stability | ΔΔG | Stability | ΔΔG | Stability | ΔΔG | Stability | ΔΔG | Stability | ΔΔG | Stability | ΔΔG | Stability | ΔΔG | Stability |
| 32 | W25C | –1.106 | Destabilizing | 0.38 | Stabilizing | –0.692 | Destabilizing | –0.55 | Destabilizing | –1.441255 | Destabilizing | –2.1 | Destabilizing | 0.86 | Destabilizing | –0.32 | Destabilizing | –0.616 | Destabilizing |
| 33 | D47H | –0.78 | Destabilizing | 0.53 | Stabilizing | –0.6 | Destabilizing | –0.671 | Destabilizing | –0.596999 | Stabilizing | –0.11 | Stabilizing | 0.51 | Stabilizing | 0.192 | Stabilizing | 0.567 | Stabilizing |
| 34 | Q49P | –0.274 | Destabilizing | –1.12 | Destabilizing | –0.28 | Destabilizing | –0.896 | Destabilizing | –0.770067 | Stabilizing | –0.41 | Destabilizing | 0.71 | Destabilizing | –0.162 | Destabilizing | –0.186 | Destabilizing |
| 35 | Q58H | –0.495 | Destabilizing | 0.79 | Stabilizing | –0.294 | Destabilizing | –0.677 | Destabilizing | –0.5396875 | Stabilizing | –0.73 | Destabilizing | 0.808 | Destabilizing | –0.018 | Destabilizing | 0.03 | Stabilizing |
| 36 | P59H | –0.001 | Destabilizing | 0.16 | Stabilizing | 0.041 | Stabilizing | –0.738 | Destabilizing | –0.5029356 | Stabilizing | –1.64 | Destabilizing | 0.86 | Destabilizing | 0.119 | Stabilizing | 0.276 | Stabilizing |
| 37 | P59A | –0.239 | Destabilizing | –0.2 | Destabilizing | –0.06 | Destabilizing | –0.852 | Destabilizing | –0.7431565 | Stabilizing | –1.86 | Destabilizing | 0.84 | Destabilizing | 0.117 | Stabilizing | 0.073 | Stabilizing |
| 38 | S86Y | –0.358 | Destabilizing | 0.33 | Stabilizing | –0.16 | Destabilizing | –0.592 | Destabilizing | –0.2277534 | Stabilizing | 0.08 | Destabilizing | 0.84 | Destabilizing | 0.744 | Stabilizing | 1.867 | Stabilizing |
| 39 | V96E | –2.489 | Destabilizing | –1.51 | Destabilizing | –2.518 | Destabilizing | –1.454 | Destabilizing | –2.522035 | Destabilizing | –1.86 | Destabilizing | 0.5 | Stabilizing | –0.153 | Destabilizing | –0.499 | Destabilizing |
| 40 | Y98C | –0.161 | Destabilizing | 0.12 | Stabilizing | 0.121 | Stabilizing | –0.885 | Destabilizing | –1.150707 | Destabilizing | –1.03 | Destabilizing | 0.7 | Destabilizing | 0.109 | Stabilizing | 0.393 | Stabilizing |
| 41 | P193L | –0.872 | Destabilizing | –0.07 | Destabilizing | –0.599 | Destabilizing | –0.126 | Destabilizing | –0.9917315 | Stabilizing | –0.73 | Destabilizing | 0.83 | Destabilizing | 0.088 | Stabilizing | 0.225 | Stabilizing |
| 42 | H194P | 0.854 | Stabilizing | –0.32 | Destabilizing | 0.749 | Stabilizing | –0.614 | Destabilizing | –0.5732749 | Stabilizing | 0.42 | Stabilizing | 0.61 | Destabilizing | 0.461 | Stabilizing | 1.045 | Stabilizing |
| 43 | S201Y | –0.41 | Destabilizing | –0.28 | Destabilizing | –0.418 | Destabilizing | –0.803 | Destabilizing | –0.5128665 | Stabilizing | 0.12 | Stabilizing | 0.58 | Destabilizing | 1.093 | Stabilizing | 1.378 | Stabilizing |
| 44 | S201F | –0.636 | Destabilizing | 0.6 | Stabilizing | –0.37 | Destabilizing | –0.558 | Destabilizing | –0.829358 | Stabilizing | 0.43 | Stabilizing | 0.61 | Destabilizing | 0.584 | Stabilizing | 0.83 | Stabilizing |
| 45 | K206R | –0.934 | Destabilizing | –0.78 | Destabilizing | –0.769 | Destabilizing | –0.384 | Destabilizing | –0.9249555 | Stabilizing | –0.14 | Destabilizing | 0.74 | Destabilizing | 0.129 | Stabilizing | 0.458 | Stabilizing |
| 46 | S220Y | –0.656 | Destabilizing | 0.3 | Stabilizing | –0.444 | Destabilizing | 0.123 | Stabilizing | –0.378394 | Stabilizing | –0.37 | Destabilizing | 0.7 | Stabilizing | 1.269 | Stabilizing | 1.86 | Stabilizing |

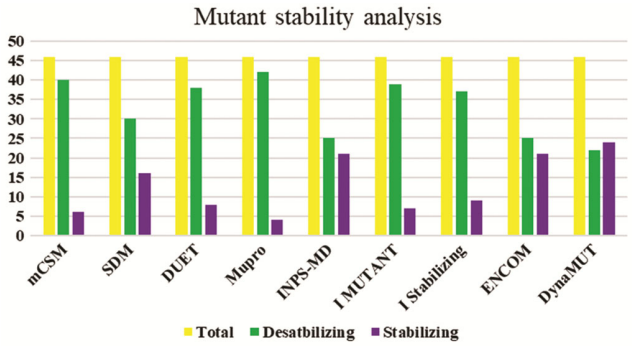


Fig. 3 — Server-based mutation stability analysis in Cx43 protein

**Conservation analysis of Cx43**

ConSurf server was used to analyze the conservative sites in the Cx43 protein. A mutation L214P was screened for conservative analysis, and the conSurf result revealed that the L214 position is subject to have more conserved at a scale of 7 (Fig. 4). From this analysis, L214P mutation was testimony for modelling and was a potent inhibitor analysis.

**Structure modelling and validation**

A crystal structure of Cx43 was not completely available in RCSB PDB; thus, a sequence of the Cx43 gene was retrieved from the Uniport database (Uniport ID: P17302) and submitted to I-TASSER web-based server. It generally retrieves template structure from the RCSB PDB library based on similar folds via a threading approach, and I-TASSER then utilizes the SPICKER program to cluster the confirmations through pairwise sequence alignment (PSA). As a result, five models generated with a confidence score from that model 1 with the best score were selected for further analysis. Cx43 was mutated by replacing the LEU at the 214$^{th}$ position

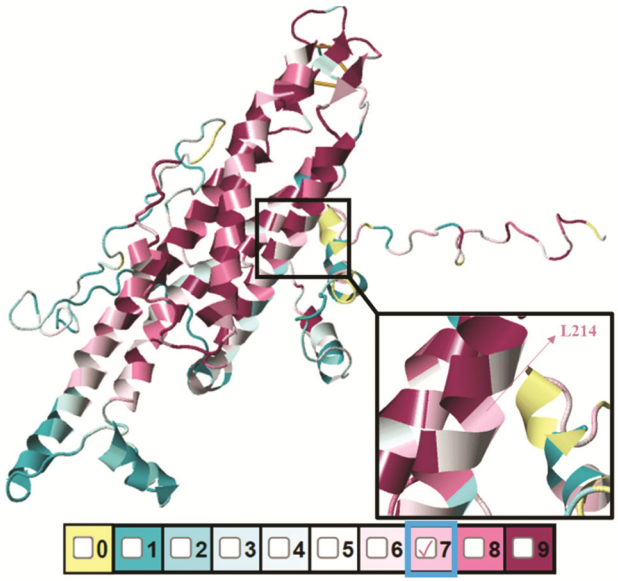


Fig. 4 — Conservative analysis of LEU at 214$^{th}$ position in native Cx43 protein

with PRO and submitted in I-TASSER (Fig. 5A & B). The native and mutant Cx43 structure was validated by the Ramachandran plot server, which obtained 94.97% and 94.362% of residues distributed in the highly preferred region of favored regions (Fig. 6).

**Molecular docking and inhibitor analysis**

In the present study, 36 compounds of interest docked with L214P mutated Cx43 protein (Table 4), which revealed the compounds Kanamycin, Ginsenoside, and Astragaloside IV shown to interact with mutated Cx43 with a maximum of 5 hydrogen bonds (Fig. 7A-C). The residues involved in the interaction are TYR155, GLY22, SER27, ASN302, ASN300, ARG293, ASN309, ARG148, LYS13 and

TYR286. Glycyrrhetinic acid, Halothane, Heptanol, Ketamine, Propofol, Quinine, pentachlorophenol, Rutaecarpine, Ascorbic acid 6-palmitate, Boldine, and Terbinafine doesn't have any hydrogen bond interactions. Other compounds showed an interaction between 1 to 4 hydrogen bonds.

AMDE result analysis revealed that high-affinity compounds Kanamycin and Astragaloside IV violated from Lipinski rule by three violations (Table 4). Ginsenoside has no violations and has high-affinity interactions of 5 hydrogen bonds with mutated Cx43 (Fig. 7B). Thus, Ginsenoside would be

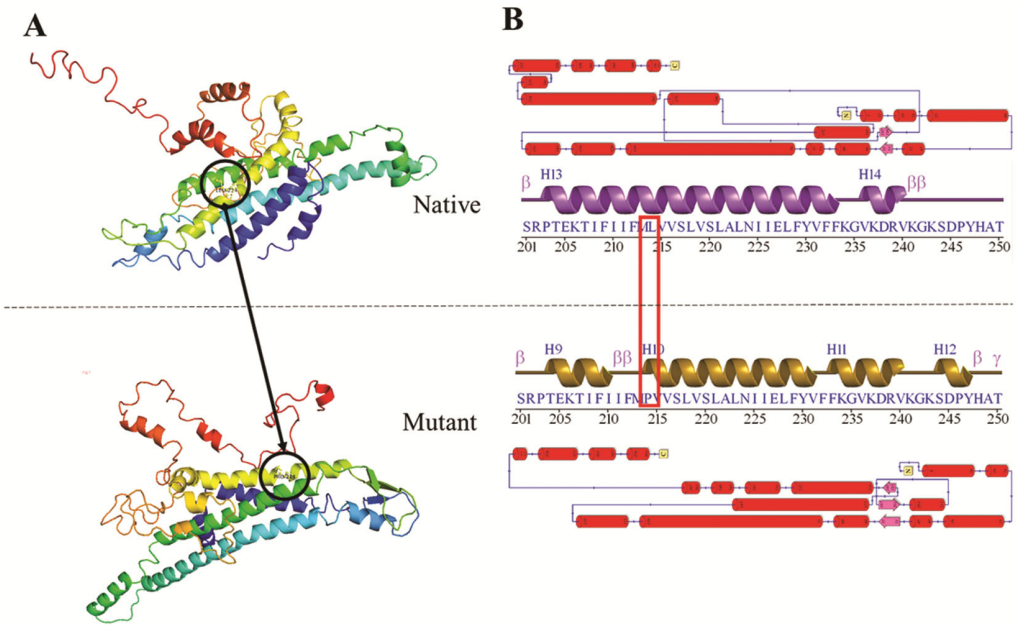


Fig. 5 — (A) 3D structure of native and mutant Cx43 protein; and (B) Secondary structural confirmation of LEU replaced with PRO at 214$^{th}$ position

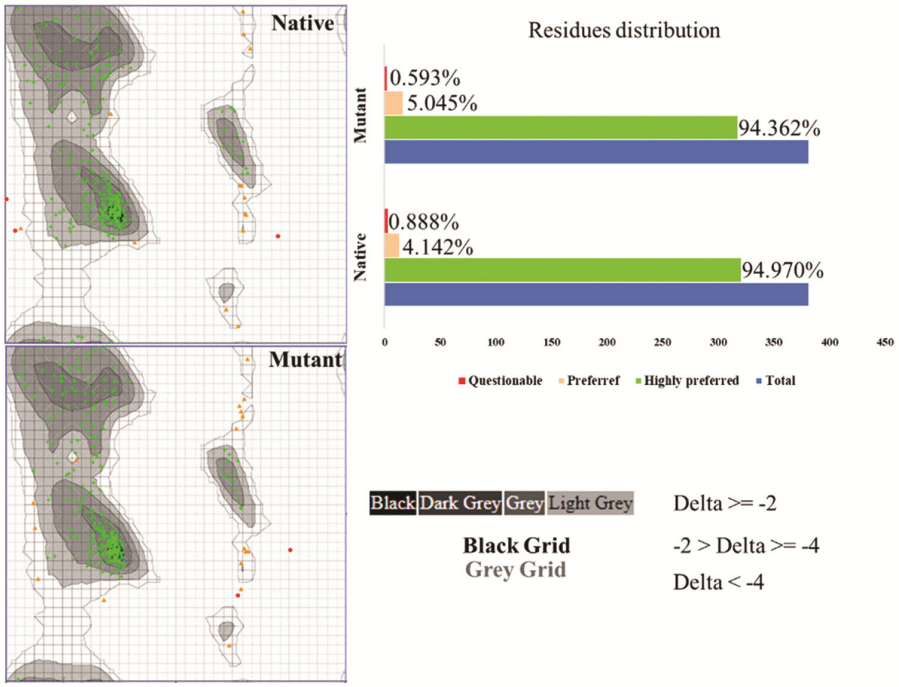


Fig. 6 — Ramachandran plot analysis of native and mutant Cx43 structure with residues distribution

Table 4 — Docking analysis and Lipinski score

| Sl. no | Inhibitors | Class | Structure | PCID | MW (g/mol) | Binding energy (kCal/mole) | H Bonds | Lipinski violation |
|---|---|---|---|---|---|---|---|---|
| 1 | 18α-glycyrrhetinic acid | Bioactive compound derivative | 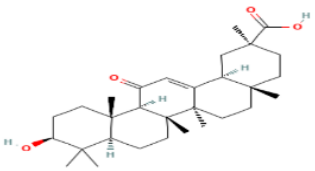 | 73398 | 470.7 | –9.5 | 2 | 1 (MLOGP>4.15) |
| 2 | 18β-glycyrrhetinic acid | Bioactive compound derivative | 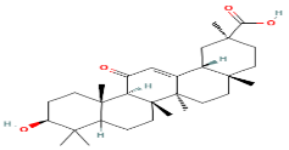 | 44435791 | 470.7 | –9.8 | 1 | 1 (MLOGP>4.15) |
| 4 | Arachidonic acid | Fatty acid | 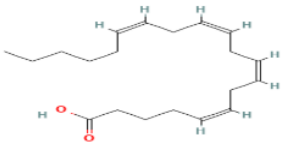 | 444899 | 304.5 | –5.5 | 1 | 1 (MLOGP>4.15) |
| 5 | Carbenoxolone | Chemical compound | 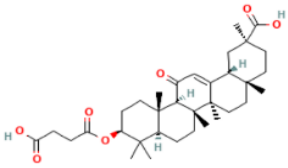 | 636403 | 570.8 | –8.9 | 4 | 2 (MW>500, MLOGP>4.15) |
| 6 | Cyclodextrins | Polysaccharide | 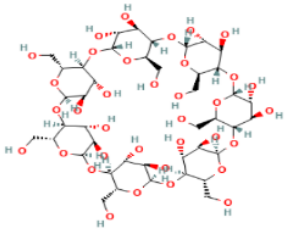 | 444041 | 1135.0 | –6.9 | 4 | 3 (MW>500, N or O>10, NH or OH>5) |
| 7 | Danegaptide | Peptide | 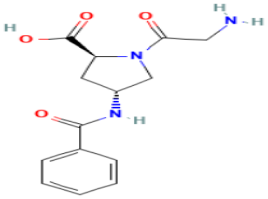 | 16656685 | 291.30 | –6.6 | 4 | 0 |
| 8 | Flufenamic acid | NSAID | 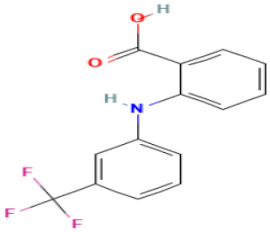 | 3371 | 281.23 | –7.9 | 2 | 0 |
| 9 | Gentamicin | Antibiotic | 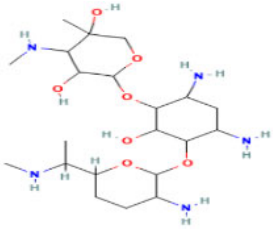 | 3467 | 477.6 | –7.1 | 4 | 2 (N or O>10, NH or OH>5) |

(*Contd.*)

Table 4 — Docking analysis and Lipinski score (*Contd.*)

| Sl. no | Inhibitors | Class | Structure | PCID | MW (g/mol) | Binding energy (kCal/mole) | H Bonds | Lipinski violation |
|---|---|---|---|---|---|---|---|---|
| 10 | Glycyrrhetinic acid | Bioactive compound | 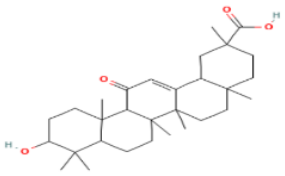 | 3230 | 470.7 | –9.8 | 0 | 1 (MLOGP>4.15) |
| 11 | Halothane | Anesthetic |  | 3562 | 197.38 | –4.4 | 0 | 0 |
| 12 | Heptanol | Chemical compound |  | 8129 | 116.20 | –4.1 | 0 | 0 |
| 13 | Kanamycin | Antibiotic | 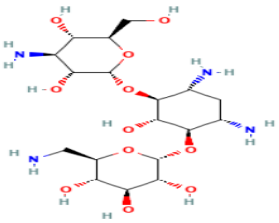 | 6032 | 484.5 | –6.0 | 5 | 2 (N or O>10, NH or OH>5) |
| 14 | Ketamine | Anesthetic | 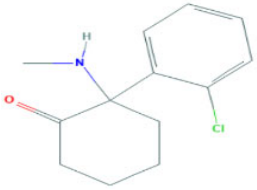 | 3821 | 237.72 | –6.9 | 0 | 0 |
| 15 | Linoleic acid | Fatty acid | 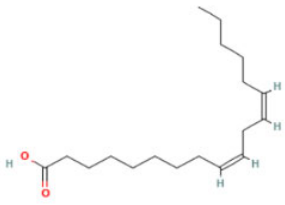 | 5280450 | 280.4 | –5.5 | 1 | 1 (MLOGP>4.15) |
| 16 | Magnesium isoglycyrrhizinate | Synthesized bioactive compound | 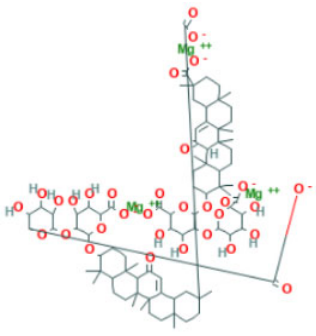 | 139032961 | 1712.7 | –9.5 | 3 | NA |

(*Contd.*)

Table 4 — Docking analysis and Lipinski score (*Contd.*)

| Sl. no | Inhibitors | Class | Structure | PCID | MW (g/mol) | Binding energy (kCal/mole) | H Bonds | Lipinski violation |
|---|---|---|---|---|---|---|---|---|
| 17 | Mefloquine | Quinolines | 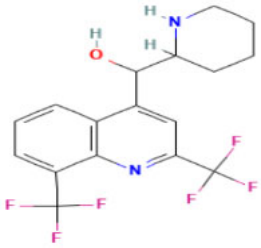 | 4046 | 378.31 | –8.7 | 2 | 0 |
| 18 | Modafinil | Chemical compound | 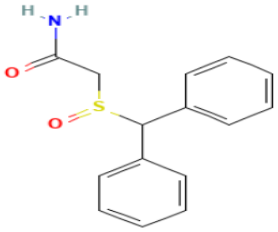 | 4236 | 273.4 | –5.1 | 2 | 0 |
| 19 | Octanol | Chemical compound |  | 957 | 130.23 | –4.5 | 1 | 0 |
| 20 | Oleic acid | Fatty acid | 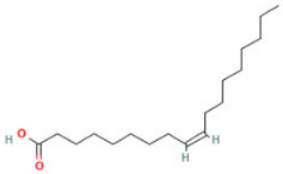 | 445639 | 282.5 | –4.6 | 1 | 1 (MLOGP>4.15) |
| 21 | Propofol | Chemical compound | 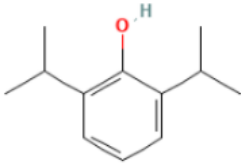 | 4943 | 178.27 | –6.2 | 0 | 0 |
| 22 | Quinine | Quinolines | 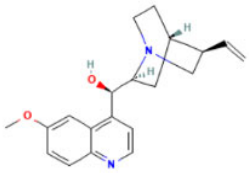 | 3034034 | 324.4 | –8.1 | 0 | 0 |
| 23 | Spermine | Polyamines | 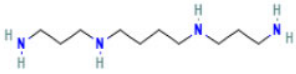 | 1103 | 202.34 | –4.0 | 1 | 0 |
| 24 | Gossypol | Bioactive compound | 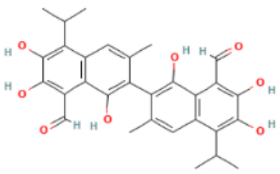 | 3503 | 518.6 | –8.5 | 3 | 2 (MW>500, NH or OH>5) |

(*Contd.*)

Table 4 — Docking analysis and Lipinski score (*Contd.*)

| Sl. no | Inhibitors | Class | Structure | PCID | MW (g/mol) | Binding energy (kCal/mole) | H Bonds | Lipinski violation |
|---|---|---|---|---|---|---|---|---|
| 25 | Salidroside | Glycosides Compound | 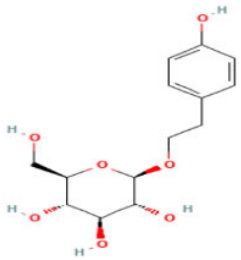 | 159278 | 300.30 | –6.7 | 3 | 0 |
| 26 | Pentachlorophenol | Chemical compound | 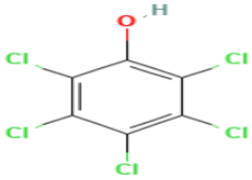 | 992 | 266.3 | –5.5 | 0 | 1 (MLOGP>4.15 |
| 27 | Ginsenoside | Steroids | 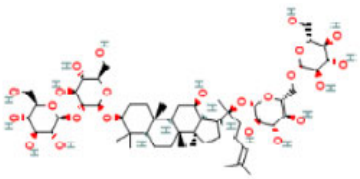 | 3086007 | 444.7 | –8.5 | 5 | 1 (MLOGP>4.15) |
| 28 | Captopril | Chemical compound | 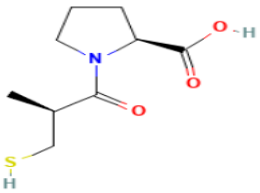 | 44093 | 217.29 | –8.0 | 1 | 0 |
| 29 | Rutaecarpine | Chemical compound | 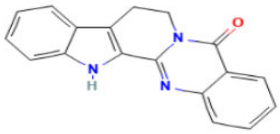 | 65752 | 287.3 | –8.7 | 0 | 0 |
| 30 | Ascorbic acid 6-palmitate | Fatty acid | 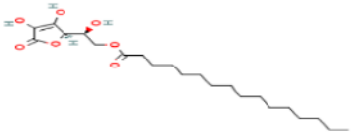 | 54680660 | 414.5 | –6.2 | 0 | 0 |

(*Contd.*)

Table 4 — Docking analysis and Lipinski score (*Contd.*)

| Sl. no | Inhibitors | Class | Structure | PCID | MW (g/mol) | Binding energy (kCal/mole) | H Bonds | Lipinski violation |
|---|---|---|---|---|---|---|---|---|
| 31 | Boldine | Alkaloid | 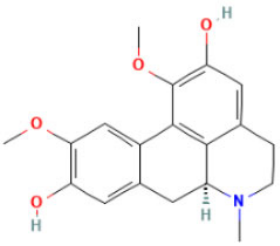 | 10154 | 327.4 | –6.5 | 0 | 0 |
| 32 | Simvastatin | Synthesized bioactive compound | 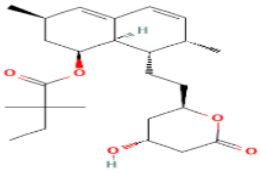 | 54454 | 418.6 | –8.8 | 1 | 0 |
| 33 | Ilimaquinone | Quinolines | 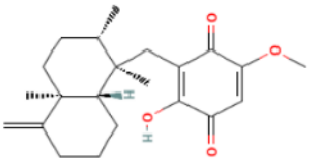 | 72291 | 358.5 | –8.4 | 1 | 0 |
| 34 | α-tocopherol | Vitamins | 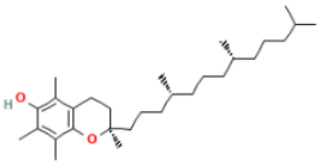 | 14985 | 430.7 | –6.0 | 1 | 1 (MLOGP>4.15) |
| 35 | Terbinafine | Allylamine derivative | 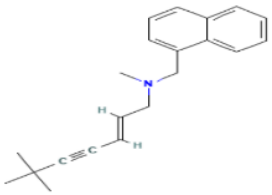 | 1549008 | 291.4 | –8.0 | 0 | 1 (MLOGP>4.15) |
| 36 | Astragaloside IV | Triterpenoid | 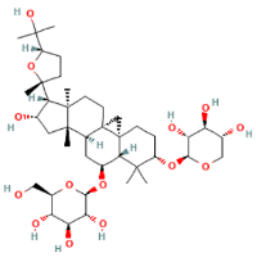 | 13943297 | 785.0 | –8.9 | 5 | 3 (MW>500, N or O>10, NH or OH>5) |
| 37 | Gallic acid | Bioactive compound | 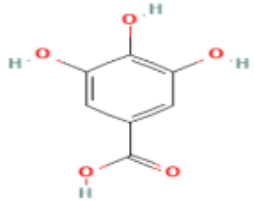 | 370 | 170.12 | –5.3 | 4 | 0 |

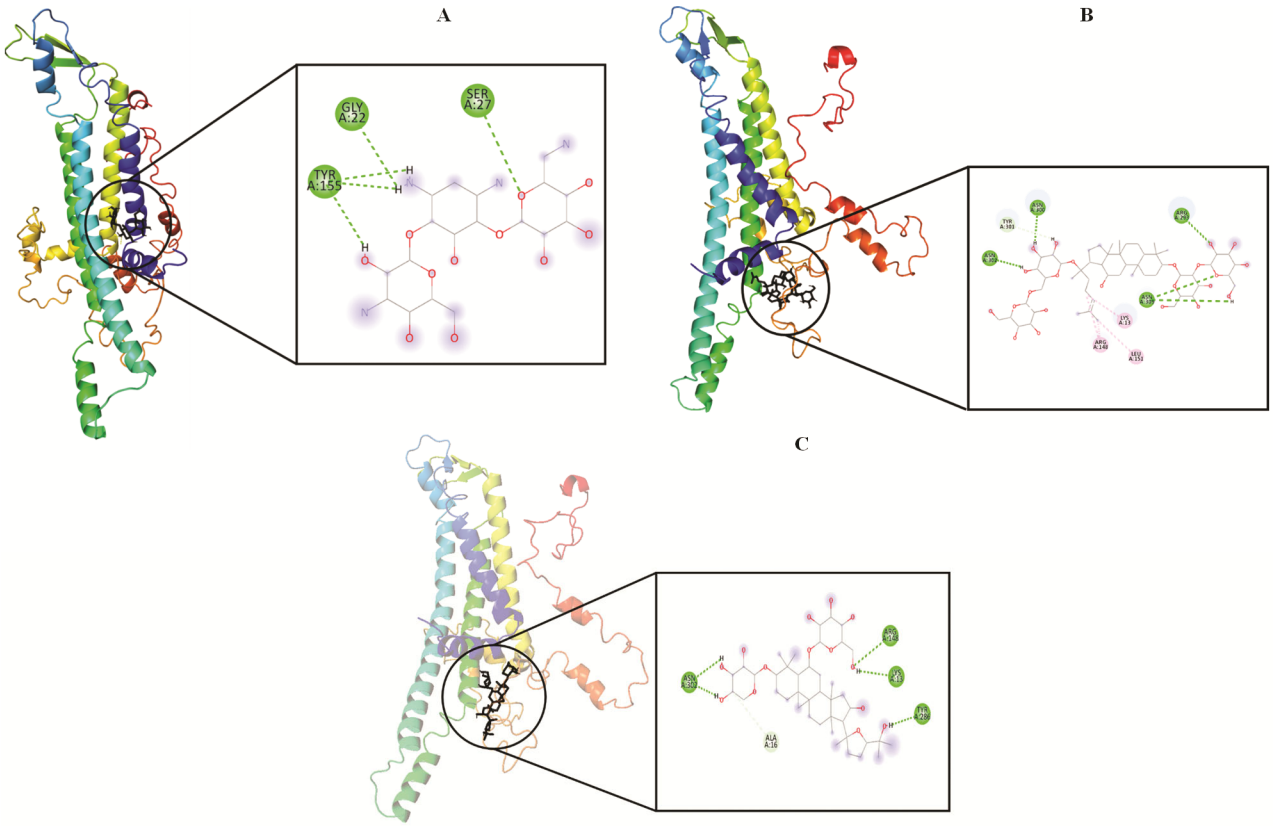


Fig. 7 — Docking analysis of (A) Kanamycin; (B) Ginsenoside; and (C) Astragaloside IV with mutated Cx43

the better compound to inhibit the L214P mutated Cx43 protein.

## Discussion

In the present study, we collected missense variants of Cx43 from different databases and literature and then identified the pathogenic mutations using five different algorithms from 219 variants. The prediction from the pathogenicity determinations server has 52 as deleterious (Table 1). Pathogenic mutations are often proven to affect protein function[22]. The deleterious mutations are analyzed for functional impact using a mutation assessor prediction server from those 46 mutations found to impact protein functions (Table 2). The protein stability of mutations was further confirmed by nine different servers, which obtained eight destabilizing mutations (Table 3). Impacts in the protein functions are primarily due to the destabilization of the protein structure[23-25].

Further, these mutations were compared with the binding pocket of Cx43, which shows L214 has been observed in the binding pocket. Which was then analyzed for a conserved position that revealed L214 kepta significant position in structural changes (Figs 4 & 6). The studies reported that an amino acid substitution at the ligand-binding site significantly alters the ligand specificity and binding affinity. Thus, inhibitors with the best binding affinity, even at mutated conditions, are important[26]. With the evidence of pathogenicity, functional impact, and structural changes, a Cx43 protein was mutated with L214P and analyzed for a potent inhibitor.

Several studies have proven that mutation at the atomic level has a severe impact on structural changes, stability, and functions of the protein[14,27].

A comparative computational approach anticipated the effect of disease-mediating missense variants in the protein structural and functional impacts[28]. In our study, the mutations such as R76H; V79F; F84C; V85G; Y177C; L214P; G60S; L11P are obtained as disease-causing and structural changes mutations in Cx43. Thus, these insights let us understand the genotype-phenotype correlation of genetic diseases related to Cx43 and assisted in scrutinizing the prioritized pathogenic mutations[29]. Based on the structural stability and binding pocket analysis, it was found that mutations at the binding pocket result to be a significant structural change. As

evidence, in (Fig. 6B), a secondary Cx43 structure (red pipeline diagram) shows two beta-strands, 18 helices, 26 helix-helix interactions, 42 beta turns, and 14 gamma turns. Three disulfides from native Cx43 were changed to 3 beta-strands, 17 helices, 19 helix-helix interactions, 50 beta turns, 23 gamma turns, and three disulfides. Research also reported that single point mutation leads to protein-misfolding or structural changes and aggregation, which is the primary cause of various diseases[30-32]. Because of mutations in Cx43, which cause various diseases, the need for drugs targeted for mutated Cx43 is recommended. A computational approach is one of the cost-efficient, time-saving and scrutinizing platforms in the field of drug discovery due to hungry for unravelling the drugs for targeted mutations in various diseases, predominantly genetic disorders.

Several studies have aimed to discover a potent drug to inhibit Cx43 protein, which Refs reports[4,5] is also depicted in (Table 4). However, no studies have yet to corroborate the inhibitors for mutated Cx43, and we aimed to analyze the interactions of Cx43 inhibitors with the native Cx43 (data not shown) and L214P mutant Cx43 protein. This analysis was obtained using the list of Cx43 inhibitors retrieved from the literature survey (Table 4). After that, Autodock vina software was used to do a virtual screening analysis on 36 Cx43 inhibitors. Among them, 30 followed the Lipinski rule of 5, from which the compound ginsenoside showed the strongest affinity (hydrogen bond: 5; binding energy: -8.5 kcal/mol) with L214P mutant Cx43 protein compared to other inhibitors (Table 4 and Fig. 7b).

Ginsenoside is a primary active compound of *Panax ginseng*, a Korean traditional medicine for longevity. There are numerous clinical studies have been conducted on various chronic diseases[33]. Also, it has been reported that ginsenosides can bind with targeted proteins in the cells, leading to beneficial effects[34]. A study reported that ginsenosides downregulated the expression of Cx43 in Bisphenol A-induced testicular toxicity[35]. In our research, ginsenosides interacted efficiently with the L214P mutant Cx43 protein. Thus, it might be a better inhibitor of native Cx43 and mutated Cx43 with a potential drug as personalized medicine.

## Conclusion

This is the first study reporting that substituting leucine at the 214$^{th}$ position with proline could be the most pathogenic mutation in disease-causing role in Cx43 protein based on the computational method. Pathogenicity of the variant was confirmed by deleterious, functional, and structural assessment of mutations. A COACH-D and CornSurf server results revealed that a residue LEU 214 significantly participated in ligand binding sites and was the most conserved residue. Further, a structure-modelled mutant with the desired variation was observed as the entire protein structure changed (Fig. 6b), which was then performed molecular docking analysis to screen potent inhibitors. The compound Kanamycin, Ginsenoside, and Astragaloside IV are better interactions with Cx43 mutants with a maximum of 5 hydrogen bonds. Ginsenoside is the only compound that follows a Lipinski rule of five. Thus, the result obtained from this study suggests that Ginsenoside would be a better potent inhibitor for native and mutant Cx43 in most genetic diseases and could therefore be a candidate for personalized medicine.

## Acknowledgement

The authors are grateful to the Vellore Institute of Technology, Vellore, for providing the facility and opportunity to carry out this work.

## Conflict of interest

All authors declare no conflict of interest.

## References

1 Sinyuk M, Mulkearns-Hubert EE, Reizes O & Lathia J, Cancer Connectors: Connexins, Gap Junctions, and Communication. *Front Oncol*, 8 (2018) 646.

2 Burendei B, Shinozaki R, Watanabe M, Terada T, Tani K & Fujiyoshi Y, Cryo-EM structures of undocked innexin-6 hemichannels in phospholipids. *Sci Adv*, 6 (2020) 3157.

3 Srinivas M, Verselis VK & White TW, Human diseases associated with connexin mutations. *Biochim Biophys Acta*, 1860 (2018) 192.

4 Natha CM, Vemulapalli V, Fiori MC, Chang CWT & Altenberg GA, Connexin hemichannel inhibitors with a focus on aminoglycosides. *Biochim Biophys Acta Mol Basis Dis*, 1867 (2021) 166115.

5 Katturajan R & Price SE, A role of connexin 43 on the drug-induced liver, kidney, and gastrointestinal tract toxicity with associated signaling pathways. *Life Sci*, 280 (2021) 119629.

6 Ishida-Yamamoto A, Erythrokeratodermia variabilis et progressiva. *J Dermatol*, 43 (2016) 280.

7 Umegaki-Arao N, Sasaki T, Fujita H, Aoki S, Kameyama K & Amagai M, Inflammatory Linear Verrucous Epidermal Nevus with a Postzygotic GJA1 Mutation Is a Mosaic Erythrokeratodermia Variabilis et Progressiva. *J Invest Dermatol*, 137 (2017) 967.

8 Wang H, Cao X, Lin Z, Lee M, Jia X & Ren Y, Exome sequencing reveals mutation in GJA1 as a cause of keratoderma-hypotrichosis-leukonychia totalis syndrome. *Hum Mol Genet*, 24 (2015) 243.

9 García IE, Prado P, Pupo A, Jara O, Rojas-Gómez D & Mujica P,Connexinopathies: a structural and functional glimpse. *BMC Cell Biol*, 17 (2016) 17.

10 Gago-Fuentes R, Fernández-Puente P, Megias D, Carpintero-Fernández P, Mateos J & Acea B, Proteomic Analysis of Connexin 43 Reveals Novel Interactors Related to Osteoarthritis. *Mol Cell Proteomics MCP*, 14 (2015) 1831.

11 Panchal NK, Bhale A, Verma VK & Beevi SS, Computational and molecular dynamics simulation approach to analyze the impactof XPD gene mutation on protein stability and function. *Mol Simul*, 46 (2020) 1200.

12 Rangasamy N, Kumar NS & Santhy KS, Computational analysis of missense variants in MMP2 gene linked with Winchester syndrome and Nodulosis-Arthropathy-Osteolysis reveals structural shift in protein-protein and protein-ligand complexes. *Meta Gene*, 29 (2021) 100931.

13 Mosaeilhy A, Mohamed MM, C GPD, El Abd HSA, Gamal R & Zaki OK, Genotype-phenotype correlation in 18 Egyptian patients with glutaric acidemia type I. *Metab Brain Dis*, 32 (2017) 417.

14 Thirumal Kumar D, Jain N, Evangeline J, Kamaraj B, Siva R & Zayed H, A computational approach for investigating the mutational landscape of RAC-alpha serine/threonine-protein kinase (AKT1) and screening inhibitors against the oncogenic E17K mutation causing breast cancer. *Comput Biol Med*, 115 (2019) 103513.

15 Katsonis P, Koire A, Wilson SJ, Hsu TK, Lua RC & Wilkins AD, Single nucleotide variations: Biological impact and theoretical interpretation. *Protein Sci Publ Protein Soc*, 23 (2014) 1650.

16 Deller MC, Kong L & Rupp B, Protein stability: a crystallographer's perspective. *Acta Crystallogr Sect F Struct Biol Commun*, 72 (2016) 72.

17 Rodrigues CH, Pires DE & Ascher DB, DynaMut: predicting the impact of mutations on protein conformation, flexibility and stability. *Nucleic Acids Res*, 2018.

18 Wu Q, Peng Z, Zhang Y & Yang J, COACH-D: improved protein–ligand binding sites prediction with refined ligand-binding poses through molecular docking. *Nucleic Acids Res*, 46 (2018) 438.

19 Honorato RV, Koukos PI, Jiménez-García B, Tsaregorodtsev A, Verlato M & Giachetti A, Structural Biology in the Clouds: The WeNMR-EOSC Ecosystem. *Front Mol Biosci*, 8 (2021) 708.

20 Ben Chorin A, Masrati G, Kessel A, Narunsky A, Sprinzak J & Lahav S, ConSurf-DB: An accessible repository for the evolutionary conservation patterns of the majority of PDB proteins. *Protein Sci Publ Protein Soc*, 29 (2020) 258.

21 Ha EJ, Lwin CT & Durrant JD, LigGrep: a tool for filtering docked poses to improve virtual-screening hit rates. *J Cheminformatics*, 12 (2020) 69.

22 Sun H & Yu G, New insights into the pathogenicity of nonsynonymous variants through multi-level analysis. *Sci Rep*, 9 (2019) 1667.

23 Shi Z & Moult J, Structural and Functional Impact of Cancer Related Missense Somatic Mutations. *J Mol Biol*, 413 (2011) 495.

24 Saffari-Chaleshtori J, Mohammad Shafiee S & Heidarian E, The effect of bilirubin on Bad, Bak, and Bim pro-apoptotic factors: A molecular dynamic simulation study. *Indian J Biochem Biophys*, 58 (2021) 236.

25 Agrawal A, Awasthi R & Kulkarni GT, A bioinformatic approach to establish P38α MAPK inhibitory mechanism of selected natural products in psoriasis. *Indian J Biochem Biophys*, 59 (2022) 165.

26 Ricatti J, Acquasaliente L, Ribaudo G, De Filippis V, Bellini M, Llovera RE, Barollo S, Pezzani R, Zagotto G, Persaud KC & Mucignat-Caretta C, Effects of point mutations in the binding pocket of the mouse major urinary protein MUP20 on ligand affinity and specificity. *Sci Rep*, 9 (2019) 300.

27 Kumar A & Purohit R, Cancer Associated E17K Mutation Causes Rapid Conformational Drift in AKT1 Pleckstrin Homology (PH) Domain. *PLoS One*, 8 (2013) 64364.

28 Agrahari AK, Sneha P, George Priya Doss C, Siva R & Zayed H, A profound computational study to prioritize the disease-causing mutations in PRPS1 gene. *Metab Brain Dis*, 33 (2018) 589.

29 Tanwar H, Kumar DT, Doss CGP & Zayed H, Bioinformatics classification of mutations in patients with Mucopolysaccharidosis IIIA. *Metab Brain Dis*, 34 (2019) 1577.

30 Wang F, Orioli S, Ianeselli A, Spagnolli G, A Beccara S & Gershenson A, All-Atom Simulations Reveal How Single-Point Mutations Promote Serpin Misfolding. *Biophys J*, 114 (2018) 2083.

31 Singh P, Yadav M, Niveria K & Verma AK, Versatility of berberine as an effective immunomodulator and chemo sensitizer against p53 mutant cell. *Indian J Biochem Biophys*, 59 (2022) 509.

32 Janani DM & Usha B, *In silico* analysis of functional non-synonymous and intronic variants found in a polycystic ovarian syndrome (PCOS) candidate gene: DENND1A. *Indian J Biochem Biophys*, 57 (2020) 584.

33 Yu SE, Mwesige B, Yi YS & Yoo BC, Ginsenosides: the need to move forward from bench to clinical trials. *J Ginseng Res*, 43 (2019) 361.

34 Kim KH, Lee D, Lee HL, Kim CE, Jung K & Kang KS, Beneficial effects of Panax ginseng for the treatment and prevention of neurodegenerative diseases: past findings and future directions. *J Ginseng Res*, 42 (2018) 23.

35 Wang L, Hao J, Hu J, Pu J, Lü Z & Zhao L, Protective Effects of Ginsenosides against Bisphenol A-Induced Cytotoxicity in 15P-1 Sertoli Cells via Extracellular Signal-Regulated Kinase 1/2 Signalling and Antioxidant Mechanisms. *Basic Clin Pharmacol Toxicol*, 111 (2012) 42.